

Absorption Physics at 351 nm in Spherical Geometry

M. C. Richardson, R. S. Craxton, J. Delettrez, R. L. Keck, R. L. McCrory, W. Seka, and J. M. Soures
Laboratory for Laser Energetics, University of Rochester, Rochester, New York 14627

(Received 9 October 1984)

Absorption and energy partitioning have been measured for spherical targets irradiated on the OMEGA facility by six beams of nanosecond 351-nm laser radiation at intensities from 10^{13} to 10^{15} W cm $^{-2}$. Efficient collisional absorption is found, in agreement with one-dimensional simulations including refraction and inhibited transport, and very low levels ($\sim 10^{-4}$) of superthermal electron production are demonstrated.

PACS numbers: 52.25.Ps, 52.50.Jm

Recent experiments with intense short-wavelength laser light have demonstrated its potential advantages for inertial-confinement fusion by direct laser irradiation. Although single-beam experiments at 1054, 526, 351, and 266 nm on planar targets show higher absorption and lower levels of fast-electron preheat for shorter wavelengths,¹⁻³ it is vital to determine the relevant scaling criteria for uniformly irradiated spherical targets. Absorption and hot-electron generation in spherical targets at intensities of 10^{14} – 10^{16} W cm $^{-2}$ have been measured at 526 nm.⁴ We report the first characterization of these quantities on spherical targets irradiated with multiple-beam 351-nm radiation.

This study used the output of the first set of six up-converted (351-nm) beams of the 24-beam OMEGA Nd:phosphate-glass laser facility,⁵ focused with single-element, 60-cm-focal-length optics ($f/3$) with respective lateral and axial pointing accuracies of 10 and 50 μ m, for the ir and uv. Estimates of the level of irradiation uniformity achieved in these experiments were made through an approach already used to determine the irradiation uniformity of all 24 beams of OMEGA in the ir (1053 nm).⁶ With the current intensity profile at 351 nm in the target plane, and with the 3% rms variance in the energies of the six beams, the overall rms variation in intensity is 50% for tangentially focused beams on targets of ~ 400 - μ m diameter.⁷

For 600–700-ps pulses in the intensity range 10^{13} – 10^{15} W cm $^{-2}$, the primary features of absorption, hot-electron generation, and thermal transport were determined on solid spherical targets of various materials with diameters of 50–400 μ m. The overall absorption was measured by a set of twenty discrete differential plasma calorimeters situated symmetrically around the target. The total absorption for CH targets of diameter 50–400 μ m is shown as a function of average incidence intensity in Fig. 1(a). All six beams were focused 8 target radii beyond target center, for which the marginal rays are tangential to the target surface. The solid and dashed lines show the absorption for these irradiation conditions predicted by, respectively, the one-dimensional version of the Eulerian code SAGE,⁸ under the assumption of a

phenomenological flux-limit parameter of $f=0.03$,⁹ and the one-dimensional Lagrangian code LILAC,¹⁰ also assuming $f=0.03$. Throughout these simulations the heat flux \mathbf{q} is given by⁹ $\mathbf{q} = -\kappa_{\text{SH}}(1 + |q_{\text{SH}}|/fq_F)^{-1}\nabla T$, where κ_{SH} and q_{SH} are the classical (Spitzer-Härm¹¹) thermal conductivity and heat flux, $q_F = n_e k T_e (k T_e / m_e)^{1/2}$, n_e , T_e , and m_e are the electron number density, temperature, and mass, respectively, and k is Boltzmann's constant. The component of absorption due to inverse bremsstrahlung is calculated with use of a self-consistent ray-tracing model, with the beam incident at tangential focus, as in the experiments, and the rays traced through the one-dimensional refractive-index distribution according to geometrical optics.^{12,13} An additional component of absorption, a small fractional ($\sim 15\%$) deposition of that energy which reaches the turning point, is also included to simulate resonance absorption. Calculations omitting this fractional energy deposition are consistent with the data in the low-to-mid intensity range, but predict less absorption than is observed above 10^{15} W cm $^{-2}$. It is likely that resonance absorption and/or the parametric decay instability occurs at 351 nm, but accompanied by deposition into electrons whose temperature is too low either to be observed from the x-ray spectrum or to present a significant preheat problem. It is also worth noting that the same value of f was used by SAGE to model uv absorption on planar targets.²

Tangential-focus conditions were used in the experiment in order to provide good irradiation uniformity for optimum coupling to the target. Higher levels of uniformity can be achieved by deliberately overfilling the target, but only at the expense of overall absorption, as is illustrated in Fig. 1(b). For comparison, absorption data obtained with 24 beams and much larger energies (~ 2 kJ) of nanosecond 1053-nm radiation are shown in Fig. 1(a). A considerable improvement in absorption with 351-nm radiation is evident. This would be even more striking if the same target sizes could have been used in both cases. However, as a result of the energy constraints in the uv, the higher-intensity shots had to be carried out with smaller-

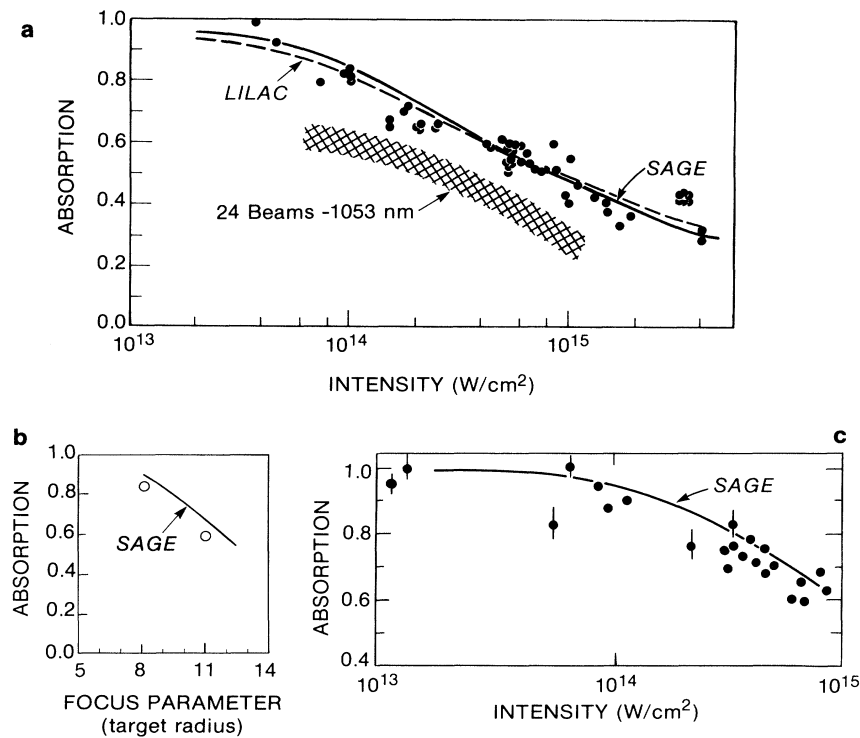


FIG. 1. (a) Absorption by polystyrene (CH) spheres as a function of intensity; also shown are 1053-nm data obtained with ~ 2 -kJ, 1-ns pulses. (b) Variation of absorption with focus parameter, the number of target radii at which each beam is focused beyond target center, for an intensity of $6 \times 10^{13} \text{ W cm}^{-2}$. (c) Absorption for Ni spheres. All SAGE and LILAC calculations were made for 200-J incident energy in 600-ps pulses.

diameter spheres. This, in turn, gives rise to shorter coronal-density scale lengths and higher refractive losses, both of which reduce the measured absorption. Higher values of absorption than reported here, at intensities above mid- $10^{14} \text{ W cm}^{-2}$, were obtained on planar targets at 351 nm,² where the scale lengths were longer. Quantitatively, SAGE predicts 50% absorption at $6 \times 10^{14} \text{ W cm}^{-2}$ for tangential focus [Fig. 1(a)], 63% for center focus (where refractive losses disappear), and 80% for planar targets.²

Absorption was also measured on spheres of other materials. Data are shown in Fig. 1(c) for nickel, together with SAGE predictions (solid curve). The measured and calculated absorption fractions are seen to be somewhat higher for the higher- Z materials (as was found in Ref. 2). It may be surprising that the difference is not greater, as the inverse-bremsstrahlung opacity is proportional to Z , but the simulations show that this is substantially compensated for by a marked steepening of the electron-density profile near the critical surface. The plasma parameters are also found to be strongly dependent on the treatment of radiation. For Fig. 1(c) a multigroup radiation-diffusion model which included Rosseland-averaged local-thermodynamic-equilibrium (LTE) opacities was used; non-LTE

radiation physics, not included in SAGE, may well be another contributing factor.¹⁴

Although the absorption data for uv irradiation can be modeled primarily on the basis of collisional absorption, it is important to laser fusion to characterize the level of any secondary, collisionless processes which may give rise to hot-electron generation. Estimates of the energy absorbed by secondary collisionless processes were made through measurements of the continuum x-ray emission in the range of 1 to 300 keV using a fifteen-channel, K -edge filter spectrometer incorporating calibrated p - i - n diodes and NaI scintillator-photomultiplier detectors.¹⁵ The data were analyzed in a self-consistent way accounting for the absorber-foil transmission near the K edge as well as at higher energies. Two- and three-temperature electron distributions have been used to fit the data by use of nonlinear least-squares-fit routines (Fig. 2). All spherical-target experiments at intensities $> 10^{14} \text{ W cm}^{-2}$ with 1053-nm radiation exhibit x-ray spectra consisting of three distinct components¹⁵: (a) thermal radiation (600–700 eV) from the critical density region, (b) a hot-electron component (5–10 keV) resulting from resonance absorption, and (c) a superhot component characteristic of very energetic electrons

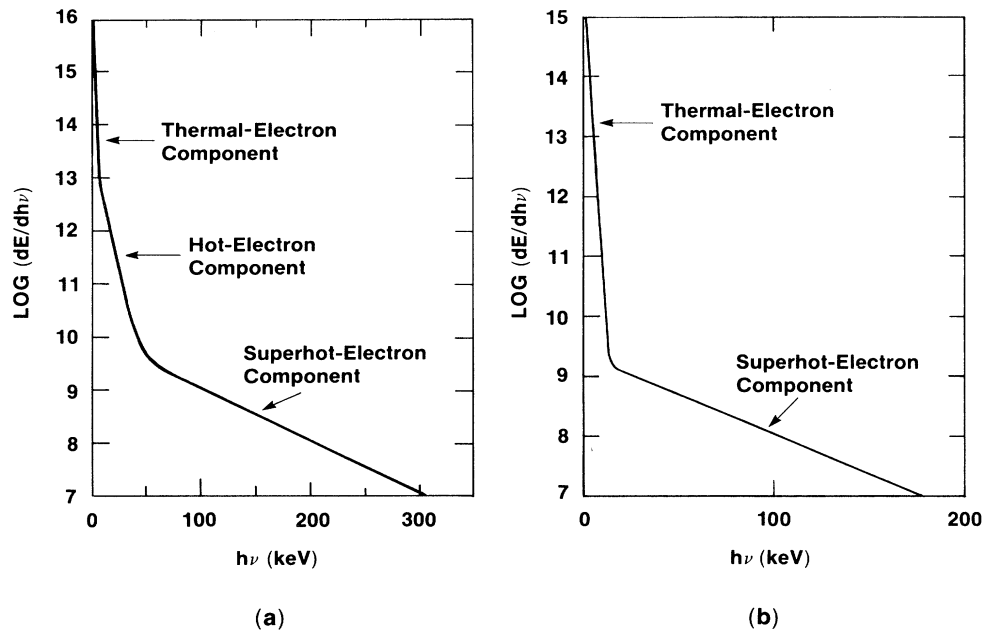


FIG. 2. X-ray continuum spectra from (a) 1053-nm and (b) 351-nm irradiated CH spheres at an intensity of $2 \times 10^{14} \text{ W cm}^{-2}$.

produced by plasmons of the $2\omega_p$ decay instability at $n_c/4$. In contrast, the continuum x-ray spectra from uv-irradiated targets [Fig. 2(b)] could only be modeled with a two-temperature electron distribution. The latter comprised a cold (thermal) component similar to that observed in the ir experiments and a second component of temperature 20–30 keV which becomes apparent only at intensities $> 10^{14} \text{ W cm}^{-2}$, corresponding to the superhot component observed in the ir experiments. The characteristic temperature of this component shows little dependence on the irradiation intensity in the range investigated.

From the fluence level of the x-ray emission an estimate of the energy partitioned into superthermal electrons can be made¹⁵ by use of a model derived by Brueckner,¹⁶ and is shown as a function of intensity in Fig. 3 for both ir and uv experiments. For ir irradiation conditions the major source of hot electrons is resonance absorption, which converts as much as 50% of the absorbed energy [or (10–15)% of the incident energy] to 5–10-keV electrons near the critical density. The energy content within the superhot component is found to be comparable for both ir and uv irradiation conditions and appears to saturate at $\sim 10^{-4}$ of the incident energy. Thus, the overall level of hot electrons sufficiently energetic to preheat fuel within the target is lower by several orders of magnitude for uv-irradiation conditions. This is in contrast to earlier results at 526 nm in spherical geometry,⁴ where ap-

proximately half of the absorbed energy was found in hot electrons produced by resonance absorption.

In an effort to determine the source of the superhot electron component, the generation efficiency of the $\frac{3}{2}$ -harmonic emission (at 234 nm) from these plasmas is also plotted in Fig. 3. It is well known that this

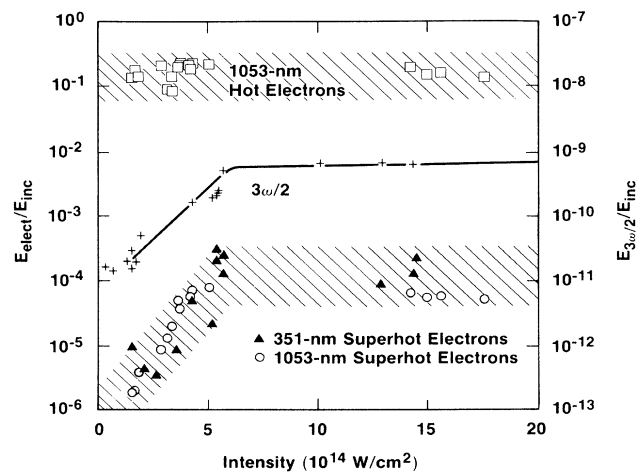


FIG. 3. Conversion fractions of incident energy (E_{inc}) into collisionless electron energy (E_{elect}) and $3\omega_0/2$ emission ($E_{3\omega/2}$) as functions of incident intensity. The data for 1053 nm are from the experiments reported in Ref. 15.

emission is related to the $2\omega_p$ decay instability at $n_c/4$.^{17,18} The close correlation between the two sets of data clearly supports the view that these two experimental signatures have a common origin in the $2\omega_p$ decay instability. Moreover, the threshold intensity of $\sim 2 \times 10^{14}$ W cm⁻² is in good agreement with that predicted¹⁸ for the $2\omega_p$ decay instability for typical coronal plasma conditions ($T_e \approx 1$ keV, and density scale length $L \approx 50$ μ m). The cause of the apparent saturation of the $2\omega_p$ decay instability is at present unclear; it may be due to changing plasma conditions (shorter scale lengths for the high-intensity shots) or to a genuine nonlinear saturation mechanism.

The efficient collisional absorption and exceedingly low levels of superthermal electron generation reported here offer considerable encouragement for direct-drive laser fusion. Future spherical uv-irradiation experiments with larger laser energies should confirm the scaling of these parameters with target size.

The authors acknowledge useful discussions with Dr. L. Goldman, Dr. S. Skupsky, Dr. K. Tanaka, and Dr. B. Yaakobi, and the technical support of R. Boni, R. Hutchison, D. Quick, and the OMEGA laser operations group during the course of these experiments. Targets used during these experiments were fabricated by the target fabrication group at the Laboratory for Laser Energetics.

This work was supported by the U. S. Department of Energy, Office of Inertial Fusion under Contract No. DE-AC08-80DP40124 and by the Laser Fusion Feasibility Project at the Laboratory for Laser Energetics which has the following sponsors: Empire State Electric Energy Research Corporation, General Electric Company, New York State Energy Research and Development Authority, Northeast Utilities Service Company, Southern California Edison Company, The Standard Oil Company (Ohio), and the University of

Rochester.

¹W. C. Mead *et al.*, Phys. Rev. Lett. **47**, 1289 (1981).

²W. Seka *et al.*, Opt. Commun. **40**, 437 (1982).

³C. Garban-Labaune *et al.*, Phys. Rev. Lett. **48**, 1018 (1982).

⁴D. C. Slater *et al.*, Phys. Rev. Lett. **46**, 1199 (1981).

⁵J. M. Soures, R. J. Hutchison, S. D. Jacobs, L. D. Lund, R. L. McCrory, and M. C. Richardson, in Proceedings of the Tenth Symposium on Fusion Engineering, Philadelphia, 1983 (to be published).

⁶M. C. Richardson, S. Skupsky, J. Kelly, L. Iwan, R. Hutchison, and R. Peck, Proc. SPEI **380**, 473 (1983).

⁷M. C. Richardson *et al.*, in Technical Digest of the Conference on Lasers and Electro-optics, 1984 (unpublished), p. 246.

⁸R. S. Craxton and R. L. McCrory, Laboratory for Laser Energetics Reports No. LLE 99 and No. LLE 108, 1980 (unpublished).

⁹R. C. Malone, R. L. McCrory, and R. L. Morse, Phys. Rev. Lett. **34**, 721 (1975).

¹⁰E. B. Goldman, Laboratory for Laser Energetics Report No. LLE 16, 1973 (unpublished).

¹¹L. Spitzer and R. Härm, Phys. Rev. **89**, 977 (1953).

¹²M. Born and E. Wolf, *Principles of Optics* (Pergamon, Oxford, 1975), 5th Ed., Sec. 3.2.1. SAGE uses Eq. (2) and LILAC uses Bouguer's formula, Eq. (7); these equations are equivalent in spherical geometry.

¹³R. S. Craxton and R. L. McCrory, J. Appl. Phys. **56**, 108 (1984).

¹⁴M. D. Rosen *et al.*, Phys. Fluids **22**, 2020 (1979).

¹⁵R. L. Keck, L. M. Goldman, M. C. Richardson, W. Seka, and K. Tanaka, Phys. Fluids **27**, 2762 (1984).

¹⁶K. A. Brueckner, Nucl. Fusion **17**, 1257 (1977).

¹⁷J. L. Bobin, M. Decroisette, B. Meyer, and Y. Vitel, Phys. Rev. Lett. **30**, 594 (1973).

¹⁸A. Simon, R. W. Short, E. A. Williams, and T. Dewandre, Phys. Fluids **26**, 3107 (1983).